



# File conversion and processing

Tony Weight

Crystallography  
**Journals**  
Online

# When a Co-editor accepts a paper

- An email is sent to the contact author of the paper
- An email is sent to the technical editor in Chester
- Files are transferred from the submission area to the paper directory for editing
- The IUCr database is updated
- The paper submission URL is closed to the author

# What files are transferred?

- Source file of the text
- Figures
- Supplementary material
- Review PDF

# Converting to SGML

- SGML = standard generalized markup language
- Structured ASCII document
- Conforms to our document type definition (DTD)
- Is an archival format
- Used for typesetting
- Used to create metadata
- Easily converted to HTML for online journals

```
<!DOCTYPE IUCR-ART PUBLIC "-//IUCr//DTD IUCr article dtd V1.1//EN"><iucr-art
pii="S0907444905017841" access="pay" version="1.1.0" docsubty="fa" crt="International Union
of Crystallography" language="0" jid="d051784" aid="hv5038"><jnlinfo editor="E.N. Baker and
Z. Dauter" name="Acta Crystallographica Section D" abbrtitle="Acta Cryst. D"
doi="10.1107/S0907444905017841" yr="2005" issn="0907-4449" coden="ABCRE6" volume="61"
lpage="1212" issue="9" fpage="1207"><fm><atl>Structure of a putative 2'-5' RNA
ligase from Pyrococcus horikoshii</atl><shortatl>2'-5' RNA
ligase</shortatl><aug><au><frm inits="P.H.">Peter H.</frm><srn index="Rehse,
P.H.">Rehse</srn></au><orf id="a"><au><frm inits="T.H.">Tahir H.</frm><srn index="Tahirov,
T.H.">Tahirov</srn></au><orf id="a"><cor email="tahir@spring8.or.jp"></cor><au-note>Current
address: Eppley Institute for Research in Cancer and Allied Diseases, LTC Room 10737A,
University of Nebraska Medical Center, 986805 Nebraska Medical Center, Omaha, NE
68198-7696, USA.</au-note><aff><oid id="a">RIKEN Harima Institute, 1-1-1 Kouto,
Mikazuki-cho, Sayo-gun, Hyogo 679-5148, <cny>Japan</cny></aff></aug><shortaug>Rehse &
Tahirov</shortaug><re yr="2005" mo="04" day="13"><acc yr="2005" mo="06" day="06"><datafile
object-type="pdb" locator="lvdX" locator-type="code">putative 2'-5' RNA ligase,
lvdX, rlvdxsf</datafile><synopsis><p>The crystal structure of a putative 2'-5'
RNA ligase from P. horikoshii was solved and compared with a Thermus
thermophilus homologue and the structurally related cyclic
phosphodiesterase.</p></synopsis><abs><p>Cyclic phosphodiesterase and 2'-5' RNA
ligase are members of a superfamily of proteins which share structural similarities even
though their homology may be very low. A putative 2'-5' RNA ligase from
Pyrococcus horikoshii has been crystallized and its X-ray crystallographic
structure determined to 2.4 Å. The protein crystallized in the orthorhombic
space group P212121, with unit-cell parameters a = 44.07, b =
45.47, c = 93.17 Å; and one protein monomer in the
asymmetric unit. The molecular-replacement probe was a 2'-5' RNA ligase from
Thermus thermophilus which shares 30% sequence identity. The
P. horikoshii RNA ligase has some structural features that have more in
common with a cyclic phosphodiesterase from Arabidopsis thaliana with which it has
no significant homology, yet an examination of the electrostatic surface potential clearly
defines its relationship to the T. thermophilus RNA ligase. However, the size of
the active-site cleft is smaller and less positively charged than that of the T.
thermophilus homologue, suggesting that the actual substrate may be smaller than that
previously postulated for the latter.</p></abs><kwdg>2'-5' RNA
ligases</kwdg></fm><bdy><sec id="secl"><st>Introduction</st><p>RNA-ligase activity
has been found in a wide range of organisms (Arn & Abelson, 1996<bbr id="bb2">). In
eukaryotic species, most RNA-ligase functions have been attributed to known RNA-processing
events such as intron removal from tRNA (Greer, Peebles <et al.>, 1983<bbr
id="bb8">) or the maturation of mitochondrial RNA of trypanosomatids (Deng <et al.>
```

Journal details

Article details

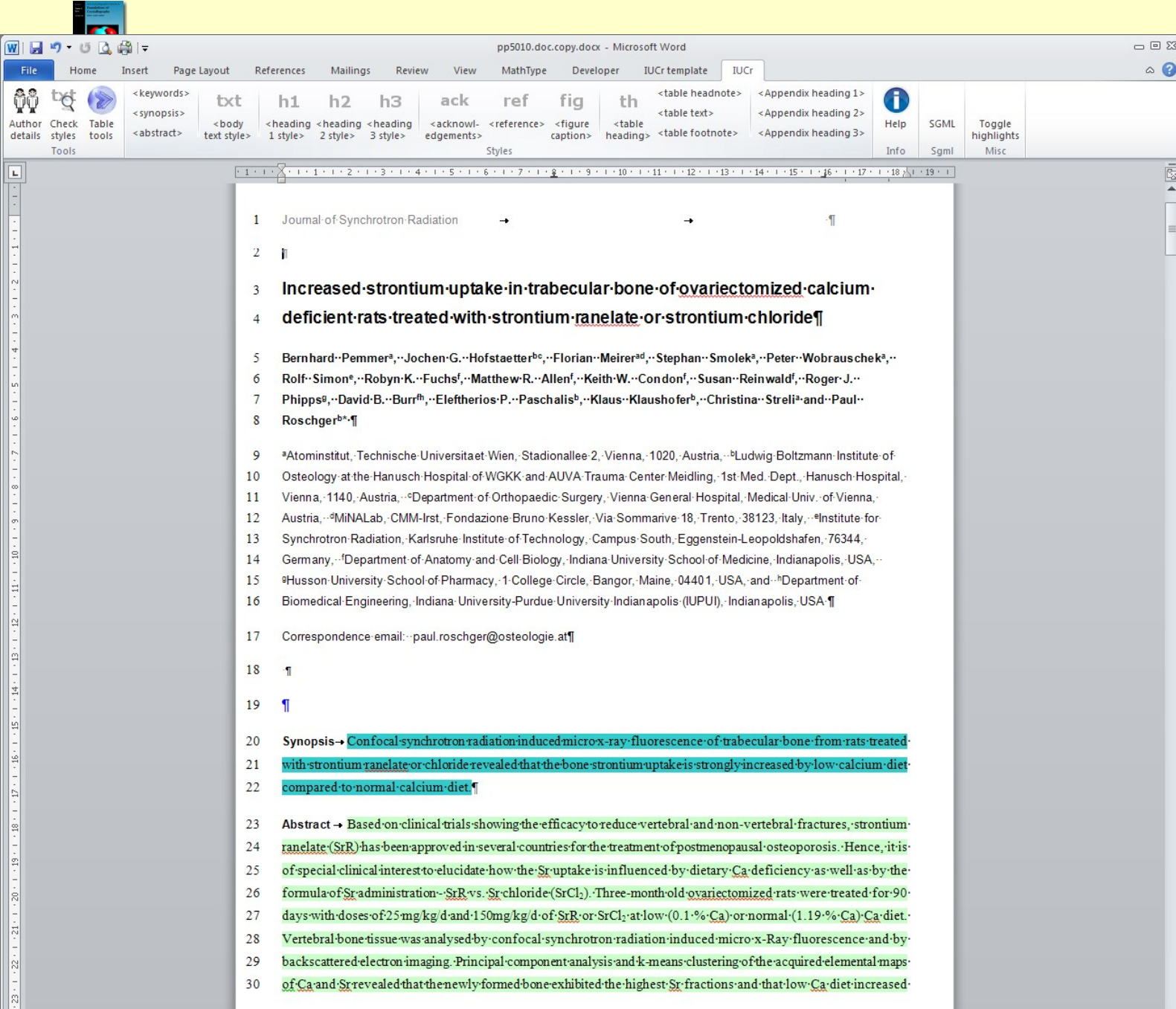
Author details

Database details

Synopsis and Abstract

Start of text

Cross references



# In-house Word template

Synopsis and Abstract automatically recognised and highlighted

Crystallography  
Journals  
Online

# In-house Word template

Keywords and a first-level heading automatically recognised and highlighted

The screenshot displays a Microsoft Word document titled 'pp5010.doc.copy.docx'. The ribbon includes 'IUCr' and 'IUCr template' tabs. The 'IUCr template' tab shows a list of styles: 'keywords', 'synopsis', 'abstract', 'body text style', 'h1', 'h2', 'h3', 'acknowledgements', 'reference', 'figure caption', 'table heading', 'table footnote', 'Appendix heading 1', 'Appendix heading 2', and 'Appendix heading 3'. The document content includes:

32 compared to SrR.

33 The study clearly shows that inadequate nutritional calcium intake significantly increases uptake of Sr in serum as well as in trabecular bone matrix. This indicates that nutritional calcium intake as well as serum Ca levels are important regulators of any Sr treatment.

36 **Keywords:** strontium ranelate; strontium chloride; dietary calcium; ovariectomized rats; SR- $\mu$ -XRF; qBEI; elemental mapping; principal component analysis; k-means clustering

37

38 **1. Introduction**

39 Strontium has been studied in context of a possible therapeutic agent for skeletal diseases for more than half a century (Marie *et al.*, 1985; McCaslin & Janes, 1959; Shorr & Carter, 1952; Skoryna, 1981; Storey, 1962; Grynias & Marie, 1990). Based on results of recent clinical trials showing reduced vertebral and non-vertebral fracture risk, strontium ranelate (SrR) is now approved in several countries for the treatment of postmenopausal osteoporosis (Reginster *et al.*, 2008). Studies on potential mechanisms for SrR anti-fracture efficacy include effects on bone microarchitecture and bone remodeling balance (Ammann *et al.*, 2007; Fuchs *et al.*, 2008a; Ma *et al.*, 2011) and Sr interaction with the calcium-sensing receptor of bone cells (Brennan *et al.*, 2009). Recent studies investigated Sr accumulation and storage in bone and whether Sr has an impact on the intrinsic material properties of bone (Li *et al.*, 2010; Roschger *et al.*, 2010). It should be emphasized that Sr with its ~two-fold atomic weight compared to Ca interferes with the measurement of bone mineral density (BMD), which is a clinically important surrogate parameter for anti-fracture effectiveness. Consequently, in Sr-treated patients changes in BMD occur not only due to changes in bone volume and/or mineral content but also due to Sr uptake, which makes reliable interpretation of osteodensitometry difficult (Bärenholdt *et al.*, 2009; Blake & Fogelman, 2007; Kendler *et al.*, 2009). Bearing in mind that in vertebrates, 99% of whole-body Ca and Sr is located in bone (Dahl *et al.*, 2001), the amount incorporated is positively correlated with serum levels of Sr as numerous studies have shown (Dahl *et al.*, 2001; Fuchs *et al.*, 2008a; Li *et al.*, 2010; Roschger *et al.*, 2010; Boivin *et al.*, 1996; Farlay *et al.*, 2005). In addition, it was recently demonstrated that Sr is preferentially located in the new bone formed during Sr treatment and only marginally located in the pre-existing bone matrix (Fuchs *et al.*, 2008a; Li *et al.*, 2010; Roschger *et al.*, 2010). Sr atoms are incorporated into the crystal lattice of the bone hydroxyapatite by ionic substitution of calcium (Li *et al.*, 2010).

58 → A recent study in ovariectomized (OVX) rats (Fuchs *et al.*, 2008a) determined the effects of high (150 mg/kg/day) and low (25 mg/kg/day) dose SrR on bone histomorphometric indices, mechanical properties and Sr uptake. Furthermore, the role of dietary calcium in modulating the effect of SrR on the skeleton was examined by feeding rats either a normal (1.19% Ca) or a low calcium diet (0.1% Ca). The concentration and distribution of Ca and Sr in cortical bone tissue of the tibial midshaft region was determined using a synchrotron radiation induced micro-X-ray fluorescence (SR- $\mu$ -XRF) method. Animals treated with high dose SrR had significantly higher Sr incorporation, regardless of Ca intake. However, compared to the normal Ca diet, the low Ca diet increased the

# In-house Word template

First and second heading levels automatically recognised and highlighted

Crystallography  
Journals  
Online

The screenshot displays a Microsoft Word document titled "pp5010.docx" with the "IUCr" template applied. The ribbon includes tabs for File, Home, Insert, Page Layout, References, Mailings, Review, View, MathType, Developer, and IUCr. The IUCr tab is active, showing a "Styles" gallery with various styles such as <keywords>, <synopsis>, <abstract>, txt, h1, h2, h3, ack, ref, fig, th, <table headnote>, <table text>, <table footnote>, <Appendix heading 1>, <Appendix heading 2>, and <Appendix heading 3>. The document content is as follows:

65 incorporation of Sr into the bone for low and high dose Sr groups. All animals treated with Sr had a higher Sr  
66 fraction at the periosteal bone surface (newly formed bone regions) compared to intracortical bone regions (older  
67 bone).¶

68 → The aim of the present study was to expand these investigations to the administration of Sr by SrCl<sub>2</sub> as well  
69 as Sr with low and normal Ca diets. A further aim was to extend the analysis for Sr uptake and distribution into the  
70 geometrical more complex trabecular bone compartment of the vertebrae, which contains bone marrow, in contrast to  
71 tibial periosteal bone. For this purpose, an advanced state of the art confocal Synchrotron radiation induced micro-X-  
72 ray fluorescence (SR-μ-XRF) technique was used. Quantitative backscattered electron imaging (qBEI) was employed  
73 to select regions of interest for SR-μ-XRF. In addition Principal Component Analysis (PCA) and K-means Clustering  
74 (KMC) were used to analyze the elemental maps and to separate regions with typical Sr to Ca fractions within the  
75 samples. This is the first time that such a technique of analysis of elemental maps has been applied to the study of  
76 bone tissue.¶

77 **2. Methods and Materials**

78 **2.1. Bone Samples¶**

79 We analyzed bone samples from the previously reported study (Fuchs *et al.*, 2008a) on Sr treatment in three-month-  
80 old OVX Sprague-Dawley rats. The animal study was approved by Indiana University's Institutional Animal Care  
81 and Use Committee. OVX rats were randomized by body mass 3 weeks post-surgery and divided into eight different  
82 treatment regimens: low (25 mg/kg/d) and high (150 mg/kg/d) dose Sr with low (0.1% Ca) and normal (1.19% Ca)  
83 dietary Ca; low (25 mg/kg/d) and high (150 mg/kg/d) SrCl<sub>2</sub> with low (0.1% Ca) and normal (1.19% Ca) dietary Ca.  
84 The Sr<sup>2+</sup> ion equivalents for Sr with the chemical formula of C<sub>12</sub>H<sub>2</sub>N<sub>2</sub>O<sub>5</sub>SSr<sub>2</sub> (513.49 g/mol) were 8.5 mg/kg/d and  
85 51 mg/kg/d, and for SrCl<sub>2</sub> with the chemical formula SrCl<sub>2</sub>·6(H<sub>2</sub>O) (266.62 g/mol) were 9.4 mg/kg/d and 56 mg/kg/d,  
86 for the low and high Sr doses, respectively. SHAM operated and untreated OVX rats fed a normal Ca diet served as  
87 controls. Animals were treated daily for 90 days. According to previously published Sr serum level data (Fuchs *et al.*,  
88 2008a) the different treatments regimens led to following mean Sr serum levels: 22.7 and 23.3 ng/mL for untreated  
89 SHAM and OVX, 2226.7 and 293.5 ng/mL for 25 mg/kg/d Sr treatment at 0.1% and 1.19% Ca diet, respectively,  
90 12611.1 and 1746.0 ng/mL for 150 mg/kg/d Sr treatment at 0.1% and 0.19% Ca diet, respectively. One L3 vertebra  
91 from each group was used for analysis, while all the measurements of the bone samples were performed blinded to  
92 the treatment (Table 1).¶

93 → Vertebrae were fixed in 70% ethanol, dehydrated through a graded series of ethanol, and embedded  
94 undecalcified in polymethylmethacrylate (PMMA). About 5 mm thick blocks containing a sagittal vertebral bone  
95 section were obtained using a low speed diamond saw (Buehler Isomet, Lake Pluff, USA). The section surfaces were  
96 ground by sandpaper and subsequently polished using a diamond suspension (3 and 1 micron grain size) on a

# In-house Word template

Figure captions automatically recognised and highlighted

pp5010.doc.copy.docx - Microsoft Word

File Home Page Layout References Mailings Review View MathType Developer IUcr template IUcr

Author details Check styles Table tools

< keywords > < synopsis > < abstract >

txt h1 h2 h3 ack ref fig th < table headnote > < table text > < table footnote > < Appendix heading 1 > < Appendix heading 2 > < Appendix heading 3 >

Info Sgml Toggle highlights Misc

1 2 3 4 5 6 7 8 9 10 11 12 13 14 15 16 17 18 19

256 **4.4. Conclusions**

257 In conclusion, dietary and serum levels of Ca are important determinants of serum Sr levels and Sr uptake into bone

258 with SrR treatment for osteoporosis. To avoid higher uptake rates of Sr and improve safety in patients being treated

259 with SrR, adequate Ca and Vitamin D intake is essential.

260 ¶

261 **Figure 1** Examples of qBEI images and the corresponding SR- $\mu$ -XRF elemental maps of calcium (Ca) and

262 strontium (Sr) based on Ca K $\alpha$  and Sr K $\alpha$  fluorescence lines, respectively, from bone samples of animals untreated

263 and treated by SrR or SrCl $_2$ : (a) untreated, (b) low Sr dose at normal Ca diet, (c) low Sr dose at deficient Ca diet, (d)

264 high Sr dose at normal Ca and (e) high Sr dose at deficient Ca. The pixel size of the SR- $\mu$ -XRF elemental maps is

265 10  $\mu$ m  $\times$  10  $\mu$ m with a depth resolution of 12  $\mu$ m at Sr K $\alpha$

266  $\alpha$  (14.2 keV). The color coded X-ray intensities (counts per second cps) are scaled from minimum to maximum.

267 qBEI shows young bone packets (less mineralized) as darker, and older bone packets as well as residual cartilage

268 (arrows) (higher mineralized) as brighter grey levels.

269 **Figure 2** Example of a PCA+KMC analysis: The scan was done on a sample (d9 of Table 1) with high dose SrR

270 treatment at deficient Ca diet.

271 (A) Score plot of principle components PC1 vs PC2 derived from a plot of Ca versus Sr intensities by linear

272 transformation exhibiting a new set mutually orthogonal axis. PC1 axis represents the direction, where Ca and Sr

273 intensities are related like, more Ca more Sr. PC2 axis represents the direction, where Ca and Sr intensities are related

274 like, more Ca less Sr and vice versa. The KMC analysis of the PCA score plot used four clusters (k=4): color-coded

275 red, green, pink and blue; X: centroid of clusters C1, C2, C3, C4; The meaning of the clusters can be explained by

276 generating binary images, where all pixels corresponding to a certain cluster are displayed in white (B).

277 (B) Binary images produced according to the cluster data: image C1 shows the distribution of pixels clustered in C1

278 (red) and corresponds to the background/bone marrow space, where both Ca and Sr concentrations are zero. Image

279 C2 (pixels from cluster C2, green) highlights areas of old bone showing a low Sr to Ca fraction, while image C3

280 (pixels clustered in C3, pink) contains pixels representing the rim region of the bone. Finally, image C4, which

281 contains all pixels of cluster C4 (blue), displays pixels of highest Sr to Ca fraction, corresponding to areas of young

282 bone.

283 **Figure 3** Influence of Ca diet on Sr uptake as quantified by cluster C4 centroid values indicated by green (normal

284 Ca diet) and red bars (deficient Ca diet), respectively, whereby differences between SrR and SrCl $_2$  are distinguished

285 by intense and light colour. The increase in Sr uptake (height of the bars) was in parallel with the increase in Sr

286 serum levels. For each sample median and range (error bars) resulting from all maps recorded are indicated.

287 Significance levels as obtained by Mann-Whitney tests: \* p < 0.05, \*\* p < 0.001, <sup>c</sup> p = 0.057.

# In-house Word template

Table caption and table footnote automatically recognised and highlighted

pp5010.doc.copy.docx - Microsoft Word

File Home Insert Page Layout References Mailings Review View MathType Developer IUCr template IUCr

Author details Check styles Table tools

<keywords> <synopsis> <abstract>

txt h1 h2 h3 ack ref fig th

<body text style> <heading 1 style> <heading 2 style> <heading 3 style> <acknowledgements> <reference> <figure caption> <table heading>

<table headnote> <table text> <table footnote>

<Appendix heading 1> <Appendix heading 2> <Appendix heading 3>

Help Info Sgml Toggle highlights Misc

284 Table 1 → Sr<sup>2+</sup> uptake of bone tissues analysed. †

experimental data			p-values between groups of maps				
sample (N)	Sr <sup>2+</sup> doses [mg/kg/d]	Ca diet [weight %]	Sr(Ca+Sr) (count rates)	vs. control	low vs. high Sr	deficient vs. normal Ca	SrR vs. SrCl <sub>2</sub>
1c	SHAM-non	1.19	0.0012				
(3)			[0.0010;0.0013]				
2c	OVX-non	1.19	0.0011	<0.01			
(4)			[0.0011;0.0012]				
3n	SrR.....8.5	1.19	0.024	<0.01			ns
(5)			[0.020;0.024]				
4n	SrCl <sub>2</sub> ...9.4	1.19	0.02148	<0.05		<0.05	
(4)			[0.018;0.023]			(<0.001)	
5d	SrR.....8.5	0.1	0.1015	<0.01		<0.05	ns
(3)			[0.094;0.109]			(<0.001)	
6d	SrCl <sub>2</sub> ...9.4	0.1	0.085	<0.01	<0.05		
(4)			[0.081;0.095]			(<0.001)	
7n	SrR.....51	1.19	0.140	<0.001	<0.01		<0.05
(4)			[0.136;0.153]			(<0.001)	
8n	SrCl <sub>2</sub> ...56	1.19	0.130	<0.05	0.1	0.05	
(8)			[0.105;0.138]			(<0.001) (<0.001)	
9d	SrR.....51	0.1	0.4252	<0.01	<0.05	<0.01	0.057
(3)			[0.418;0.435]			(<0.001) (<0.001)	
10d	SrCl <sub>2</sub> ...56	0.1	0.3528				
(4)			[0.322;0.378]				

285 †

286 Data shown are median and range [min; max] obtained from the elemental maps performed for each bone tissue sample; N= number of maps per sample; Calcium diet: 1.19% is normal, 0.1% is deficient; Sr(Ca+Sr) values of cluster C4 (region of highest Sr fractions) representing the newly formed bone matrix (see also Fig 2); p-values between the groups of single Sr(Ca+Sr) outcomes of each bone sample; p-values in brackets (...) means that the data of SrR and SrCl<sub>2</sub> samples were correspondingly pooled. †

288

289

The screenshot shows a Microsoft Word document titled "pp5010.doc.copy.docx". The ribbon includes File, Home, Insert, Page Layout, References, Mailings, Review, View, MathType, Developer, IUCr template, and IUCr. The IUCr template ribbon is active, showing options for keywords, synopsis, abstract, body text style, heading styles (h1, h2, h3), acknowledgements, reference, figure caption, table heading, table text, table footnote, and appendix headings. The document content includes:

297 Acknowledgements → This work was supported by the European Community Research Infrastructure Action  
298 under the FP6 "Structuring the European Research Area" ("Integrating Activity on Synchrotron and Free Electron  
299 Laser Science" (IA-SFS) RII3-CT-2004-506008), by the AUVA (Austrian Workers' Compensation Board), the  
300 WGKK (Vienna Health Insurance Fund), and a research grant from the Alliance for Better Bone Health. Further we  
301 thank G. Dinst, S. Thon, Ph. Messmer, and D. Gabriel for careful sample preparations, qBEJ and EDX  
302 measurements.

303  
304

305 **References**

306 Ammann, P., Badoud, J., Barraud, S., Dayer, R., & Rizzoli, R. (2007). *Journal of Bone and Mineral Research* **22**,  
307 1419-1425.

308 Bärenholdt, O., Kolthoff, N., & Nielsen, S. P. (2009). *Bone* **45**, 200-206.

309 Blake, G. M., & Fogelman, I. (2007). *J Clin Densitom* **10**, 259-265.

310 Boivin, G., Deloffre, P., Perrat, B., Panczer, G., Boudeulle, M., Mauras, Y., Allain, P., Tsouderos, Y., & Meunier, P.  
311 J. (1996). *Journal of Bone and Mineral Research* **11**, 1302-1311.

312 Brennan, T. C., Rybchyn, M. S., Green, W., Atwa, S., Conigrave, A. D., & Mason, R. S. (2009). *British Journal of*  
313 *Pharmacology* **157**, 1291-1300.

314 Dahl, S. G., Allain, P., Marie, P. J., Mauras, Y., Boivin, G., Ammann, P., Tsouderos, Y., Delmas, P. D., &  
315 Christiansen, C. (2001). *Bone* **28**, 446-453.

316 Farlay, D., Boivin, G., Panczer, G., Lalande, A., & Meunier, P. J. (2005). *Journal of Bone and Mineral Research* **20**,  
317 1569-1578.

318 Fratzl-Zelman, N., Roschger, P., Gourrier, A., Weber, M., Misof, B., Loveridge, N., Reeve, J., Klaushofer, K., &  
319 Fratzl, P. (2009). *Calcified Tissue International* **85**, 335-343.

320 Fuchs, R. K., Allen, M. R., Condon, K. W., Reinwald, S., Miller, L. M., McClenathan, D., Keck, B., Phipps, R. J., &  
321 Burr, D. B. (2008a). *Osteoporos Int* **19**, 1331-1341.

322 Fuchs, R. K., Allen, M. R., Condon, K. W., Reinwald, S., Miller, L. M., McClenathan, D., Keck, B., Phipps, R. J., &  
323 Burr, D. B. (2008b). *Osteoporosis International* **19**, 1815-1817.

324 Grynpas, M. D., & Marie, P. J. (1990). *Bone* **11**, 313-319.

325 Janssens, K., Proost, K., & Falkenberg, G. (2004). *Spectrochim Acta B* **59**, 1637-1645.

326 Kanngießer, B., Malzer, W., & Reiche, I. (2003). *Nuclear Instruments and Methods in Physics Research Section B:*  
327 *Beam Interactions with Materials and Atoms* **211**, 259-264.

328 Kendler, D. L., Adachi, J. D., Josse, R. G., & Slosman, D. O. (2009). *Osteoporos Int* **20**, 1101-1106.

# In-house Word template

Acknowledgements and References automatically recognised and highlighted


Crystallography  
Journals  
Online

# Conversion of Word file to SGML

- Text is converted to SGML
- Mathematical equations are converted to TeX format using MathType
- References are checked against databases  
e.g. Crystallography Journals Online, PubMed
- Resulting SGML file is saved in the paper directory

# Conversion of LaTeX file to SGML

- SGML conversion starts automatically once paper is accepted
- References are checked against databases  
*e.g.* Crystallography Journals Online, PubMed
- Resulting SGML file is saved in the paper directory



# Filtering the SGML

- Adds fixed spaces between possible units and values
- Double spaces are removed
- Unit symbols are altered, *e.g.* seconds becomes s
- Table attributes are changed, *e.g.* entries are aligned left
- Sections, figures and tables are numbered
- Cross references citations to figures, tables, schemes, equations and footnotes
- Checks for uncited figures, tables, schemes, equations and footnotes

The screenshot shows a window titled "wiucrbbbr" with a menu bar containing "Start", "Remove tag", "Replace selected Text", and "Save & Exit". The main text area contains XML code for a journal article, including DOCTYPE declarations, journal information, author names, and a synopsis. Below the main text, there is a section for "Constructed citation replacements. Note: not always correct." which lists various citation formats for the same article. At the bottom, there is a section for "Contents of <bibl> tags" showing the XML code for the bibliography entries.

```

<!DOCTYPE IUCR-ART PUBLIC "-//IUCr//DTD IUCr article dtd V1.1//EN"><!--ArborText, Inc., 1988-1998, v.4002--><?P
ub EntList alpha bull copy rArr sect trade plusmn deg thetas le lang rang z-Lt equiv Omega><?Pub Inc><?created by I2
s version 0.96 Fri Jul 29 21:03:42 2011><iucr-art version="1.1.0" jid="s113068" aid="vv5017" docsubty="fa" crt="Internation
al Union of Crystallography" language="0"><jnlinfo name="Journal of Synchrotron Radiation" yr="2011" issue="1" volume
="67" issn="0909-0495" fpage="000" lpage="000"><fm><atl>Fluorescence detection of white-beam x-ray absorption aniso
tropy: towards element sensitive projections of local atomic structure</atl><shortatl>Projections of local atomic structur
e</shortatl><aug><au><fnm>P.</fnm><snm index="Korecki, P.">Korecki</snm></au><orf id="a"><cor email="pawel.kore
cki@uj.edu.pl" correspondence="yes" contact="yes"></cor><au><fnm>M.</fnm><snm index="Tolkiehn, M.">Tolkiehn</sn
m></au><orf id="b"><au><fnm>K. M.</fnm><snm index="D\c{a}browski, K. M.">Da&lgrave;&sect;browski</snm></au><o
rf id="a"><au><fnm>D. V.</fnm><snm index="Novikov, D. V.">Novikov</snm></au><orf id="b"><aff><oid id="a">Institute
of Physics, Jagiellonian University, Reymonta 4,30-059 Krak&oacute;w, <cny>Poland</cny></aff><aff><oid id="b">DES
Y, Notkestra&szlig;e 85, D-22603 Hamburg, <cny>Germany</cny></aff></aug><shortaug>P. Korecki et al.</shortaug><r
e day="07" mo="06" yr="2011"><acc day="29" mo="07" yr="2011"><synopsis><p>
A method for a direct measurement of x-ray projections of the atomic structure is described. Projections of the atomic s

```

Constructed citation replacements. Note: not always correct.

```

<empty>
Abrahams <it>et al.</it>, 1966<bbr id="bb1">
Abrahams <it>et al.</it> (1966<bbr id="bb1">
Abrahams, Hamilton & Reddy, 1966<bbr id="bb1">
Abrahams, Hamilton & Reddy (1966<bbr id="bb1">
Adams <it>et al.</it>, 1998<bbr id="bb2">
Adams <it>et al.</it> (1998<bbr id="bb2">
Adams, Novikov, Hiort, Materlik & Kossel, 1998<bbr id="bb2">

```

Contents of <bibl> tags

```

<bibl>
<bb id="bb1">Abrahams, S. C., Hamilton, W. C. & Reddy, J. M. (1966). <it>J. Phys. Chem. Solids</it>, <b>27</b>, 1013&ndash;1018.</bb>
<bb id="bb2">Adams, B., Novikov, D. V., Hiort, T., Materlik, G. & Kossel, E. (1998). <it>Phys. Rev. B</it>, <b>57</b>, 7526&ndash;7534.</b>
<bb id="bb3">Antoine, J.-P., Demanet, L., Jacques, L. & Vanderghyest, P. (2002). <it>Appl. Comput. Harmon. Anal.</it> <b>13</b>, 177&ndash;
200.</bb>
<bb id="bb4">Barton, J. J. (1988). <it>Phys. Rev. Lett.</it> <b>61</b>, 1356&ndash;1359.<?PMID10038773></bb>
<bb id="bb5">Berg, J. C. van den, (ed & ) (2004). <it>Wavelets in Physics</it>. Cambridge University Press.</bb>

```

# Reference filter program

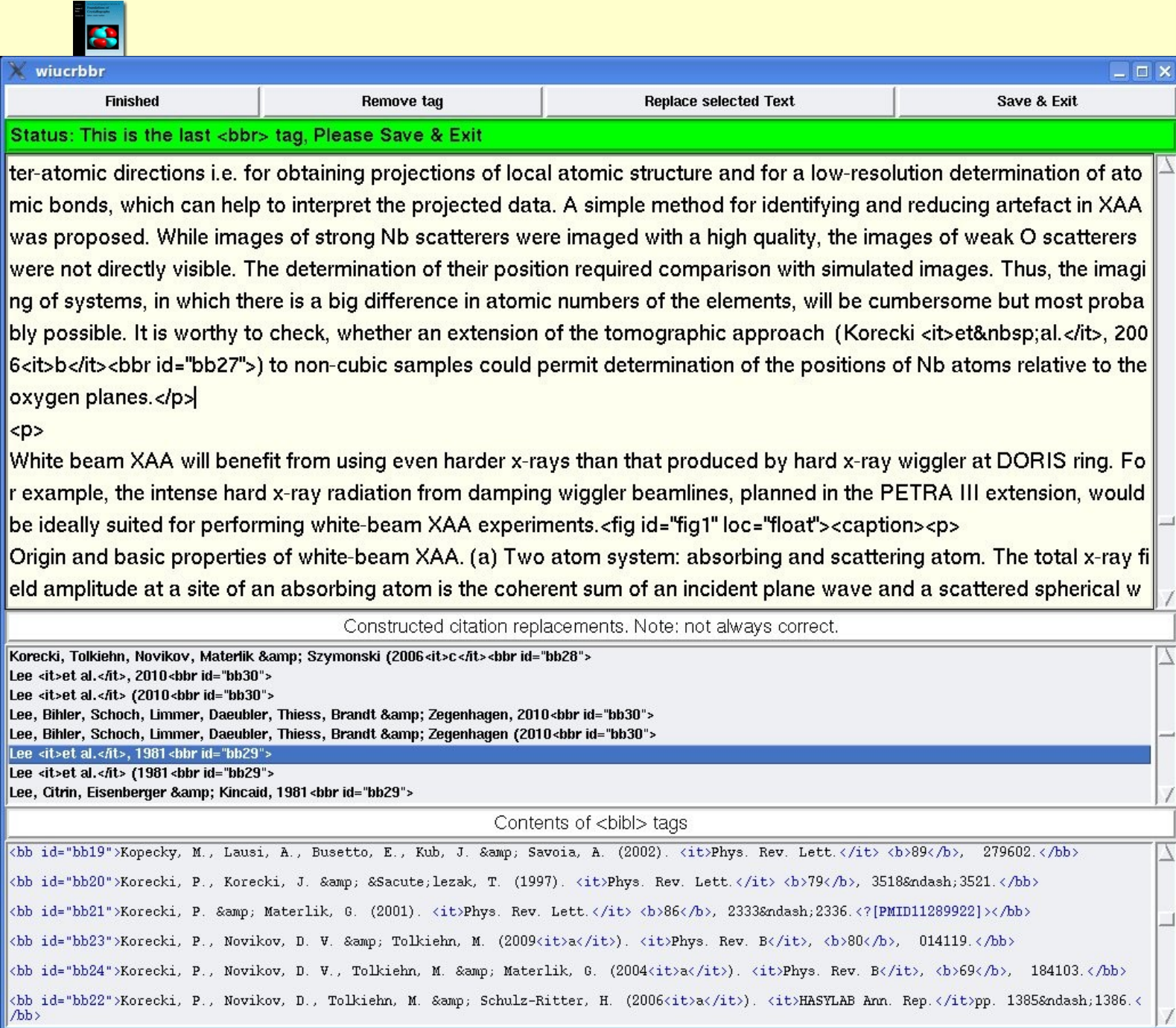
Checks citations  
In text against  
references

# Reference filter program

If a citation cannot be matched it is highlighted

NO EXACT MATCH, for ion of calcium (Li <it>et al.</it>, 2009 ...please use Replace selected Text button

Sr has an impact on the intrinsic material properties of bone (Li <it>et al.</it>, 2010<bbr id="bb15">, Roschger <it>et al.</it>, 2010<bbr id="bb22">). It should be emphasized that Sr with its ~two fold atomic weight compared to Ca interferes with the measurement of bone mineral density (BMD), which is a clinically important surrogate parameter for antifracture effectiveness. Consequently, in Sr treated patients changes in BMD occur not only due to changes in bone volume and / or mineral content but also due to Sr uptake, which makes reliable interpretation of osteodensitometry difficult (B&auml;renholdt <it>et al.</it>, 2009<bbr id="bb2">, Blake & Fogelman, 2007<bbr id="bb3">, Kendler <it>et al.</it>, 2009<bbr id="bb14">). Bearing in mind that in vertebrates, 99% of whole body Ca and Sr is located in bone (Dahl <it>et al.</it>, 2001<bbr id="bb6">), the amount incorporated is positively correlated with serum levels of Sr as numerous studies have shown (Dahl <it>et al.</it>, 2001<bbr id="bb6">, Fuchs <it>et al.</it>, 2008<it>a</it><bbr id="bb9">, Li <it>et al.</it>, 2010<bbr id="bb15">, Roschger <it>et al.</it>, 2010<bbr id="bb22">, Boivin <it>et al.</it>, 1996<bbr id="bb4">, Farlay <it>et al.</it>, 2005<bbr id="bb7">). In addition, it was recently demonstrated that Sr is located in the bone formed during treatment and only marginally located in the pre-existing bone matrix (Fuchs <it>et al.</it>, 2008<it>a</it><bbr id="bb9">, Li <it>et al.</it>, 2010<bbr id="bb15">, Roschger <it>et al.</it>, 2010<bbr id="bb22">). Sr atoms are incorporated into the crystal lattice of the bone hydroxyapatite by ionic substitution of calcium (Li <it>et al.</it>, 2009<bbr id="bb1">).</p></div><div data-bbox="216 568 542 591" data-label="Text"><p>Constructed citation replacements. Note: not always correct.</p></div><div data-bbox="2 598 273 743" data-label="Text"><p>Kendler <it>et al.</it> (2009<bbr id="bb14"><br>Kendler, Adachi, Josse & Slosman, 2009<bbr id="bb14"><br>Kendler, Adachi, Josse & Slosman (2009<bbr id="bb14"><br>Li <it>et al.</it>, 2010<bbr id="bb15"><br>Li <it>et al.</it> (2010<bbr id="bb15"><br>Li, Paris, Siegel, Roschger, Paschalis, Klaushofer & Fratzi, 2010<bbr id="bb15"><br>Li, Paris, Siegel, Roschger, Paschalis, Klaushofer & Fratzi (2010<bbr id="bb15"><br>Ma <it>et al.</it>, 2011<bbr id="bb16"></p></div><div data-bbox="313 752 444 774" data-label="Text"><p>Contents of <bibl> tags</p></div><div data-bbox="2 781 739 937" data-label="Text"><p><bbr id="bb14">Kendler, D. L., Adachi, J. D., Josse, R. G. & Slosman, D. O. (2009). <it>Osteoporos. Int.</it> <b>20</b>, 1101&ndash;1106.<? [PMID19266136]></bbr><br><bbr id="bb15">Li, C., Paris, O., Siegel, S., Roschger, P., Paschalis, E. P., Klaushofer, K. & Fratzi, P. (2010). <it>J. Bone Miner. Res.</it> <b>25</b>, 968&ndash;975.<? [PMID19874195]></bbr><br><bbr id="bb16">Ma, Y. L., Zeng, Q. Q., Porras, L. L., Harvey, A., Moore, T. L., Shelbourn, T. L., Dalsky, G. P., Wronski, T. J., Aguirre, J. I., Bryant, H. U. & Sato, M. (2011). <it>Endocrinology</it>, <b>152</b>, 1767&ndash;1778.<? [PMID21343258]></bbr><br><bbr id="bb17">Marie, P. J., Garba, M. T., Hott, M. & Miravet, L. (1985). <it>Miner. Electrolyte Metab.</it> <b>11</b>, 5&ndash;13.<? [PMID3974537]></bbr></p></div></div>



wiucrbbr

Finished Remove tag Replace selected Text Save & Exit

Status: This is the last <bbr> tag, Please Save & Exit

ter-atomic directions i.e. for obtaining projections of local atomic structure and for a low-resolution determination of atomic bonds, which can help to interpret the projected data. A simple method for identifying and reducing artefact in XAA was proposed. While images of strong Nb scatterers were imaged with a high quality, the images of weak O scatterers were not directly visible. The determination of their position required comparison with simulated images. Thus, the imaging of systems, in which there is a big difference in atomic numbers of the elements, will be cumbersome but most probably possible. It is worthy to check, whether an extension of the tomographic approach (Korecki *et al.*, 2006) to non-cubic samples could permit determination of the positions of Nb atoms relative to the oxygen planes.

White beam XAA will benefit from using even harder x-rays than that produced by hard x-ray wiggler at DORIS ring. For example, the intense hard x-ray radiation from damping wiggler beamlines, planned in the PETRA III extension, would be ideally suited for performing white-beam XAA experiments.

Origin and basic properties of white-beam XAA. (a) Two atom system: absorbing and scattering atom. The total x-ray field amplitude at a site of an absorbing atom is the coherent sum of an incident plane wave and a scattered spherical wave

Constructed citation replacements. Note: not always correct.

Korecki, Tolkiehn, Novikov, Materlik & Szymanski (2006) *et al.*, 2010  
Lee *et al.*, 2010  
Lee *et al.* (2010)  
Lee, Bihler, Schoch, Limmer, Daeubler, Thiess, Brandt & Zegenhagen, 2010  
Lee, Bihler, Schoch, Limmer, Daeubler, Thiess, Brandt & Zegenhagen (2010)  
Lee *et al.*, 1981  
Lee *et al.* (1981)  
Lee, Citrin, Eisenberger & Kincaid, 1981

Contents of < bibl > tags

< bib id="bb19">Kopecky, M., Lausi, A., Busetto, E., Kub, J. & Savoia, A. (2002). *Phys. Rev. Lett.* **89**, 279602.  
< bib id="bb20">Korecki, P., Korecki, J. & Sacute, lezak, T. (1997). *Phys. Rev. Lett.* **79**, 3518–3521.  
< bib id="bb21">Korecki, P. & Materlik, G. (2001). *Phys. Rev. Lett.* **86**, 2333–2336. <?PMID11289922>  
< bib id="bb23">Korecki, P., Novikov, D. V. & Tolkiehn, M. (2009). *Phys. Rev. B*, **80**, 014119.  
< bib id="bb24">Korecki, P., Novikov, D. V., Tolkiehn, M. & Materlik, G. (2004). *Phys. Rev. B*, **69**, 184103.  
< bib id="bb22">Korecki, P., Novikov, D., Tolkiehn, M. & Schulz-Ritter, H. (2006). *HASYLAB Ann. Rep.* pp. 1385–1386.

# Reference filter program

All citations have been checked

File is saved and is ready for editing